



# Sutural Morphology in the Craniofacial Skeleton: A Descriptive Microcomputed Tomography Study in a Swine Model

FABIO SAVOLDI <sup>1,2</sup>, JAMES K. H. TSOI <sup>1\*</sup>, CORRADO PAGANELLI,<sup>2</sup> AND JUKKA P. MATINLINNA<sup>1</sup>

<sup>1</sup>Dental Materials Science, Division of Applied Oral Sciences and Community Dental Care, Faculty of Dentistry, The University of Hong Kong, Prince Philip Dental Hospital, Sai Ying Pun, Hong Kong

<sup>2</sup>Department of Orthodontics, Dental School, University of Brescia, Brescia, Italy

## ABSTRACT

Sutures are greatly involved in both normal craniofacial growth and developmental anomalies. Having clear parameters for defining their morphology is fundamental to properly investigate their physiological or pathological development. However, the current literature is lacking of well-defined methods for the assessment of these structures. This study performed a comprehensive microcomputed tomography ( $\mu$ CT) analysis of a swine model evaluating morphological variation of sutures in different skull regions. Seventy-two suture samples were removed from one swine (*Sus scrofa*), approximately 9–12-month-old. Each sample was analyzed with  $\mu$ CT in the parallel (PAR) and perpendicular (PER) plane with respect to the bone surface. Suture width ( $S_w$ ), linear obliteration index ( $LOI$ ), and linear interdigitation index ( $LII$ ) were calculated in each of the two reference planes, and sutures were categorized in four types ( $S_t$ ). Parameters were compared among the facial, craniofacial, and cranial region. Description of the main morphological parameters was provided, and differences were found between the parallel and perpendicular planes.  $S_t$  varied depending on the skull region, with simple sutures more represented in the cranial region.  $LII$  in the perpendicular plane decreased from facial to craniofacial and cranial region.  $S_w$  in the parallel plane decreased from facial and craniofacial to cranial region. In the swine model, the sutural width, linear interdigitation, and suture type were related to distinct skull regions. The suture type was introduced to allow a better morphological characterization of sutures as 3D structures. Clear definition of sutural parameters is important for appropriate description of these complex structures. *Anat Rec*, 302:2156–2163, 2019. © 2019 American Association for Anatomy

**Key words:** anatomy; craniofacial; structure; bone; computerized tomography; distraction osteogenesis

Sutural growth is regulated by genetic and environmental factors, and the morphology of individual sutures is related to the characteristics of local mechanical

stimuli, showing a process of developmental adaptation (Herring, 2008). However, anomalies may occur and sutural development may be altered in different areas,

Additional Supporting Information may be found in the online version of this article.

Grant sponsor: Research Grants Council of Hong Kong; Grant number: Hong Kong PhD Fellowship.

\*Correspondence to: James K. H. Tsoi, 1/F, The Prince Philip Dental Hospital, Sai Ying Pun, Hong Kong. Fax: +852 2548 9464. E-mail: jkhtsoi@hku.hk

Received 25 February 2019; Revised 16 April 2019; Accepted 17 May 2019.

DOI: 10.1002/ar.24230

Published online 21 August 2019 in Wiley Online Library (wileyonlinelibrary.com).

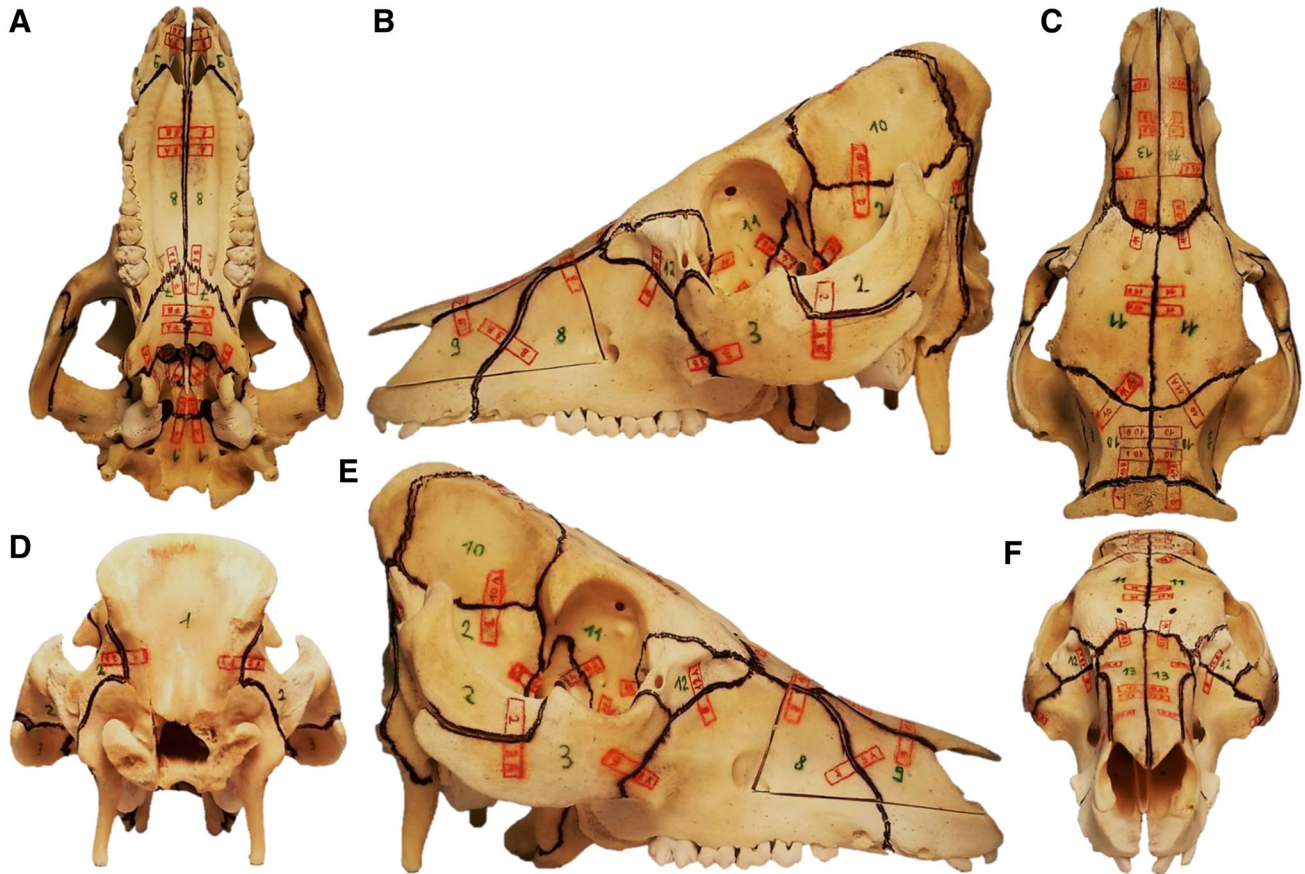


Fig. 1. Occlusal (A), lateral left (B), cranial (C), caudal (D), lateral right (E), and frontal (F) view of the swine skull. Sutures are outlined in black, bones are numbered in green, and specimens are marked in red. Several sutures cannot be identified from the external view of the skull.

including the palate (Cohen Jr, 2002) and other facial regions (Hassan and Lees, 2014).

On the other hand, extrinsic distraction forces can induce sutural remodeling (Hou et al., 2007), which can be utilized in treatments such as the rapid maxillary expansion (Trindade-Suedam et al., 2016) or the maxillary protraction (Tome et al., 2016). Furthermore, sutural ossification and anatomy are important in craniofacial surgery when premature ossification occurs in case of craniosynostosis (Tahiri et al., 2014). For these reasons, the knowledge of sutural architecture also has clinical relevance, especially when techniques such as sutural distraction osteogenesis (SDO) are adopted (Park and Yoon, 2011).

The anatomical characteristics of sutures have been historically studied in forensic medicine, introducing concepts such as interdigitation for measuring their complexity (Jayaprakash and Srinivasan, 2013), and ossification for estimating their maturation (Mann et al., 1991). However, studies have mainly focused on sutures of the calvaria (Hershkovitz et al., 1997), and there is a dearth of more comprehensive analyses of the entire sutural system, which is composed of more than forty sutures (Savoldi et al., 2018). Biomechanical investigations have also contributed to develop measurements of the linear complexity of sutures (Rafferty and Herring, 1999), and to quantify the amount of ossification (Maloul et al., 2010). However, both

the assessment methods and the definitions of such parameters have shown differences among studies (Persson and Thilander, 1977; Hershkovitz et al., 1997; Rafferty and Herring, 1999; Maloul et al., 2013).

That said, the relevance of sutural morphology in craniofacial biology supports the importance to adopt unambiguous definitions and clear methods for their analysis. Overall, microcomputed tomography ( $\mu$ CT) has demonstrated to be a fundamental instrument for the evaluation of sutures, allowing detailed ultrastructural analysis and quantitative assessments both in physiological (Korbmacher et al., 2007) and pathological conditions (Sherick et al., 2000; Corega et al., 2010; Nowaczewska et al., 2015).

Thus, the aim of the present study was to describe the sutural anatomical parameters by using  $\mu$ CT including the entire skull of a swine model. Furthermore, variations of the sutural morphology in different skull regions were analyzed.

## MATERIALS AND METHODS

### Specimen Preparation and Experimental Setup

One skull of an approximately 9–12-month-old male swine (*Sus scrofa*) was purchased from the market as food for human consumption. Procedures were carried out in agreement with local regulations for animal research and no ethical approval was necessary for the analyzed material.

Specimens were removed across the suture and perpendicular to it from 36 sutures (Fig. 1). Two specimens were selected for each suture (A and B) for a total of 72 specimens. Sutures were removed with a hand-piece air-turbine with water supply (PrestoAcqua<sup>®</sup> II, Nakanishi, Japan). The specimen size was  $\approx 20 \times 5 \text{ mm}^2$  and the thickness was determined according to local anatomy. Specimens were stored at  $-20^\circ\text{C}$  and thawed at room temperature ( $25^\circ\text{C}$ ) for 8 hr in saline solution before  $\mu\text{CT}$ .

### Acquisition of Anatomical Data

Each specimen was scanned using  $\mu\text{CT}$  at  $640 \times 512$  pixel, 80 kV, 100 mA, 1 degree rotation step, and  $25 \mu\text{m}$  pixel (SkyScan<sup>®</sup>, 1172, Bruker, Billerica, MA). Two solid volumes of hydroxyapatite with bone mineral density of 0.25 and  $0.75 \text{ g/cm}^3$  were used to calibrate the gray scale.

Measurements were taken in the parallel plane (PAR, parallel to the bone surface and to the plane of the sutural interface) and in the perpendicular plane (PER, perpendicular to the bone surface and to the plane of the sutural interface), both centered in the middle of the suture in the axial plane (AX, the plane of the sutural interface) (Fig. 2).

The length of the suture ( $l$ , mm) and the width of the specimen ( $l_0$ , mm) were measured, and the linear interdigitation index ( $LII$ , mm/mm) was calculated (Fig. 2):

$$LII_{\text{PAR}} = l_{\text{PAR}}/l_{0\text{PAR}} \quad (1)$$

and

$$LII_{\text{PER}} = l_{\text{PER}}/l_{0\text{PER}}. \quad (2)$$

The integer ( $\Delta$ ) closer to the average  $LII$  was utilized to create four interdigitation categories, that is, I (low), II (moderate–low), III (moderate–high), and IV (high). Sutures were categorized in four types ( $S_i$ ): A1, A2, B1, and B2 (Fig. 2):

$$(\text{if } LII_{\text{PAR}} < \Delta, A); (\text{if } LII_{\text{PAR}} \geq \Delta, B) \quad (3)$$

and

$$(\text{if } LII_{\text{PER}} < \Delta, 1); (\text{if } LII_{\text{PER}} \geq \Delta, 2). \quad (4)$$

The sutural width ( $S_w$ , mm) was calculated as the average among four measurements along the suture line ( $l$ ).

The length of obliterated suture ( $l_{\text{ob}}$ , mm) was calculated as the sum of the obliterated segments (defined as no radio-transparent area between the two bony fronts) along the suture line ( $l$ ), and the linear obliteration index ( $LOI$ , mm/mm) was calculated (Fig. 2):

$$LOI_{\text{PAR}} = l_{\text{obPAR}}/l_{0\text{PAR}} \quad (5)$$

and

$$LOI_{\text{PER}} = l_{\text{obPER}}/l_{0\text{PER}}. \quad (6)$$

Measurements were obtained with graphical software [ImageJ (Schneider et al., 2012)]. Part of the measurements was also used in a separate study on the biomechanical characterization of the same specimens (Savoldi et al., 2017).

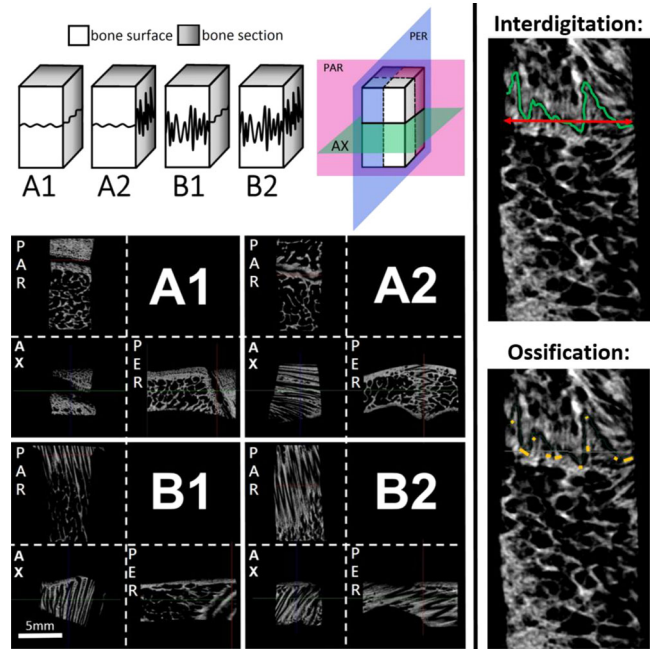


Fig. 2. (Upper left) Classification of the sutures in the four types ( $S_i$ ), according to the parallel (PAR, purple), perpendicular (PER, blue), and axial (AX, green) plane. Example sutures: almost linear both planes (A1); highly interdigitated on PER but almost linear on PAR (A2); highly interdigitated on PAR but almost linear on PER (B1); highly interdigitated on both (B2). (Lower left) Microcomputed tomography images of (A1) temporo-zygomatic, (A2) naso-nasal, (B1) fronto-nasal, and (B2) ethmoido-nasal sutures. (Right) Example of the sphenotemporal suture; interdigitation measurement illustrating the specimen width (red) and the suture length (green); respective obliteration measurement illustrating the obliterated segments (orange), and the suture length (green).

### Statistical Analysis

Sutures were divided into “facial” (i.e., connecting two facial bones), “craniofacial” (i.e., connecting a facial bone with a cranial bone), and “cranial” (i.e., connecting two cranial bones), identifying three skull regions ( $R$ ).

Data were analyzed using statistical software (SPSS<sup>®</sup>, IBM, Armonk, New York) with significance  $\alpha = 0.05$ . Data distribution was assessed with the Shapiro–Wilk test, and median and interquartile range (IQR) were calculated for each parameter. Differences in  $LII$ ,  $LOI$ , and  $S_w$  between A and B samples, and between PAR and PER of the same specimen were analyzed with the Wilcoxon signed ranks test for paired values. The  $\chi^2$ -test was used to compare suture type ( $S_i$ ) with  $R$ . The Kruskal–Wallis test with the Mann–Whitney *post hoc* test (the Bonferroni correction of significance  $\alpha = 0.05/n$ ,  $\alpha = 0.017$ ) was used to compare  $LII$ ,  $LOI$ , and  $S_w$ , respectively to  $R$ .

### RESULTS

$LII_{\text{PAR}}$  had higher median values (2.30, IQR = 2.02) compared to  $LII_{\text{PER}}$  (3.55, IQR = 3.46), with significant differences within the same suture ( $P = 0.015$ ).  $LOI_{\text{PAR}}$  (0.02, IQR = 0.05) showed higher median values than  $LOI_{\text{PER}}$  (0.03, IQR = 0.08) as well ( $P = 0.012$ ), and  $S_w$  PAR

TABLE 1. Descriptive statistics

	<i>R</i>	<i>S<sub>t</sub></i>	<i>S<sub>w</sub></i> <sub>PAR</sub>	<i>S<sub>w</sub></i> <sub>PER</sub>	<i>LII</i> <sub>PAR</sub>	<i>LII</i> <sub>PAR</sub>	<i>LII</i> <sub>PER</sub>	<i>LII</i> <sub>PER</sub>	<i>LOI</i> <sub>PAR</sub>	<i>LOI</i> <sub>PER</sub>
			(µm)	(µm)	(mm/mm)	(degree)	(mm/mm)	(degree)	(mm/mm) (%)	(mm/mm) (%)
Median			286	176	2.30		3.55		1.7	3.1
IQR			235	155	2.02		3.46		5.3	7.9
Inferior nasal conchae-maxillary	F	A2	212	95	1.15	I	4.57	IV	13.3	8.3
Maxillo-lacrimal	F	A2	539	174	2.36	II	8.32	IV	3.8	3.1
Maxillo-maxillary	F	A2	440	117	2.46	II	4.95	IV	2.5	1.0
Maxillo-nasal	F	A2	365	268	2.30	II	4.53	IV	4.5	6.3
Maxillo-palatal	F	A2	478	104	1.95	I	3.72	III	0.0	11.3
Maxillo-premaxillary	F	A1	676	506	1.10	I	1.55	I	0.0	0.0
Maxillo-vomer	F	B2 & A2	291	117	2.53	II	4.95	IV	10.6	7.5
Maxillo-zygomatic	F	B2	261	281	8.92	IV	6.01	IV	7.5	11.1
Naso-nasal	F	A2	422	177	1.08	I	3.26	III	0.0	2.6
Naso-premaxillary	F	A1	751	479	1.03	I	1.30	I	0.0	0.0
Palato-palatal	F	B2	164	172	10.75	IV	5.09	IV	9.9	10.8
Palato-vomer	F	A1	201	131	1.07	I	1.03	I	5.0	0.0
Zygomatico-lacrimal	F	B2	253	204	7.12	IV	5.74	IV	3.6	9.9
Ethmoido-inferior nasal conchae	CF	A2	281	233	1.77	I	3.73	III	0.0	0.0
Ethmoido-maxillary	CF	A2	764	220	1.81	I	4.59	IV	0.0	13.3
Ethmoido-nasal	CF	B1	385	464	10.50	IV	1.17	I	0.0	1.6
Ethmoido-palatal	CF	A2	322	165	2.34	II	6.23	IV	6.5	6.8
Ethmoido-vomer	CF	A1	186	161	2.02	II	1.80	I	7.9	6.5
Fronto-lacrimal	CF	B2	239	136	4.71	IV	4.95	IV	9.6	11.6
Fronto-maxillary	CF	A2 & B2	448	338	3.27	III	3.88	III	0.3	1.4
Fronto-nasal	CF	B2	231	355	10.26	IV	6.70	IV	0.6	0.0
Lacrino-ethmoidal	CF	B1 & A1	394	312	3.24	III	2.36	II	0.0	0.0
Palato-sphenoidal	CF	A2	692	208	1.16	I	3.70	III	0.0	0.0
Spheno-vomer	CF	A2 & B2	167	139	3.15	III	3.88	III	1.3	2.5
Temporo-zygomatic	CF	A1	631	483	1.03	I	1.28	I	0.0	0.0
Ethmoido-frontal	C	A1	440	149	1.08	I	1.76	I	2.0	6.9
Ethmoido-sphenoidal <sup>a</sup>	C	B2	157	133	4.65	IV	5.16	IV	2.4	3.1
Fronto-frontal	C	A1	120	95	1.05	I	1.12	I	0.9	7.8
Fronto-parietal	C	A1	204	176	1.26	I	1.02	I	1.0	3.8
Fronto-sphenoidal	C	A1	205	149	2.79	II	2.77	II	4.8	17.2
Occipito-parietal	C	A1	303	294	1.20	I	1.07	I	0.0	0.0
Occipito-sphenoidal <sup>a</sup>	C	A1	410	463	1.07	I	1.09	I	0.0	0.0
Occipito-temporal	C	B2 & A2	258	293	3.06	III	3.39	III	6.2	3.1
Parieto-parietal	C	A1	154	185	1.25	I	1.04	I	3.8	0.0
Parieto-temporal	C	A1 & A2	206	135	2.99	II	3.33	III	1.4	6.2
Spheno-temporal	C	A1	174	151	2.30	II	1.91	I	11.2	22.1

Description of craniofacial region (*R*), suture type (*S<sub>t</sub>*), sutural width (*S<sub>w</sub>*), linear interdigitation index on the parallel (*LII*<sub>PAR</sub>) and perpendicular (*LII*<sub>PER</sub>) plane, and linear obliteration index on the parallel (*LOI*<sub>PAR</sub>) and perpendicular (*LOI*<sub>PER</sub>) plane, of each analyzed suture.

Abbreviation: IQR, interquartile range; F, facial; CF, craniofacial; C, cranial.

<sup>a</sup> The occipito-sphenoidal and ethmoido-sphenoidal articulations are synchondroses and not syndesmoses as sutures.

(286 µm, IQR = 235 µm) presented lower median values than *S<sub>w</sub>*<sub>PER</sub> (176 µm, IQR = 155 µm) instead (*P* < 0.001) (Table 1).

The average *LII* was 3.3 and a  $\Delta = 3.0$  was adopted as cutoff. Thus, interdigitation categories were defined as I (from 1.0 to <2.0), II (from 2.0 to <3.0), III (from 3.0 to <4.0), and IV ( $\geq 4.0$ ).

Data were not normally distributed and nonparametric tests were performed.

No differences were found between specimens A and B for both *LII*<sub>PAR</sub> (*P* = 0.934), *LII*<sub>PER</sub> (*P* = 0.642), *LOI*<sub>PAR</sub> (*P* = 0.175), *LOI*<sub>PER</sub> (*P* = 0.861), *S<sub>w</sub>*<sub>PAR</sub> (*P* = 0.499), and *S<sub>w</sub>*<sub>PER</sub> (*P* = 0.192).

Differences were found in the *LII*<sub>PER</sub> relative to *R* (*P* = 0.001), with values decreasing from facial (4.35,

IQR = 2.55), to craniofacial (3.48, IQR = 2.22), to cranial (1.74, IQR = 1.88) (Fig. 3). Differences were also found in the *S<sub>w</sub>*<sub>PAR</sub> relative to *R* (*P* = 0.004), with values decreasing from facial (388 µm, IQR = 224 µm) and craniofacial (394 µm, IQR = 256 µm), to cranial (239 µm, IQR = 115 µm) (Fig. 3). Both *LOI*<sub>PAR</sub> (*P* = 0.130) and *LOI*<sub>PER</sub> (*P* = 0.214) did not show significant differences among the respective skull regions (Fig. 3). Significant differences were found among the three regions relative to suture type (A1, A2, B1, and B2) (*P* < 0.001) (Table 2). Most of the sutures in the facial (50.0%) and craniofacial (41.7%) regions were of A2 type, whereas in the cranial region they were mainly A1 (77.3%) (*P* < 0.001).

A graphical 2D representation of the results presented in Figure 3, and the  $\mu$ CT images of each sample are available in the Appendix.



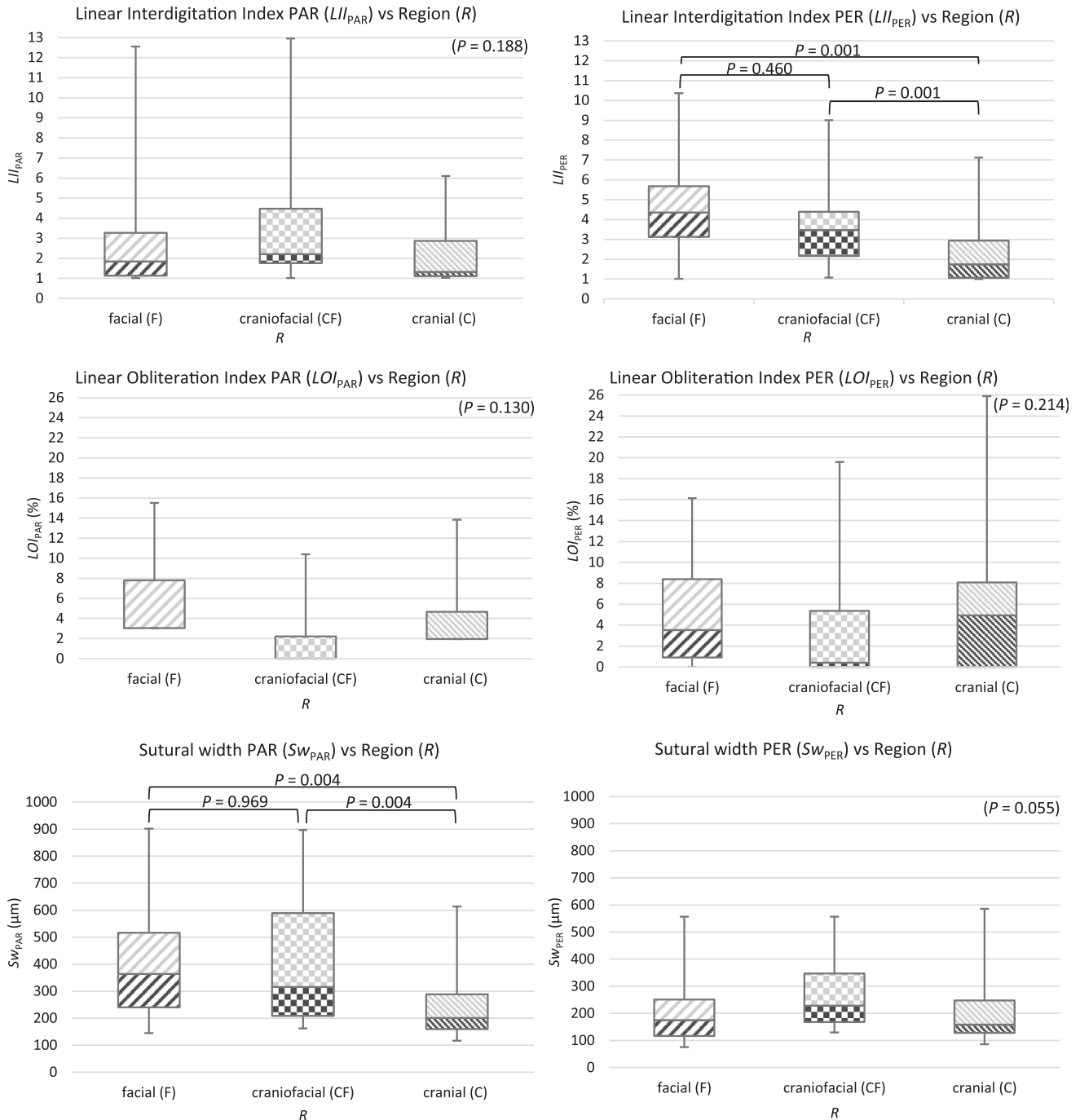


Fig. 3. Values of the linear interdigitation index ( $LII$ ), linear obliteration index ( $LOI$ ), and sutural width ( $S_w$ ) in the parallel (PAR) and perpendicular (PER) plane, relative to the skull region (R). The box top represents the upper quartile, the middle line represents the median, and the box bottom represents the lower quartile. Different shadings represent different regions of the skull. Whiskers represent maximum and minimum.

## DISCUSSION

The sutural interdigitation was defined by Rafferty et al. with the interdigitation index ( $II$ ) as the course of the suture from the endocranial to the ectocranial surface divided by the shortest distance between the suture's openings on the two surfaces (Rafferty and Herring, 1999), ergo measured on the cross-section and corresponding to the  $LII_{PER}$  described in the present study. The histological analysis offers high

image resolution, and may allow identification of the two bony margins of the sutural interface. Accordingly, in a previous histological analysis the length of the suture was measured along one suture margin (Burn et al., 2010), rather than along the course of the suture in the middle of the interface. By using this method, although bone irregularities may lead to overestimate the interdigitation, Burn et al. reported  $LII_{PER}$  values ranging from 3.61 to 7.66 for the

**TABLE 2. Distribution of suture type in the skull: Prevalence of suture types in each region**

		Suture type ( $S_i$ )				Total
		A1	A2	B1	B2	
Region ( $R$ )	facial	6	13	0	7	26
		23.1%	50.0%	0.0%	26.9%	100.0%
	craniofacial	21.4%	52.0%	0.0%	43.8%	36.1%
		5	10	3	6	24
	cranial	20.8%	41.7%	12.5%	25.0%	100.0%
		17.9%	40.0%	100.0%	37.5%	33.3%
	Total	17	2	0	3	22
		77.3%***	9.1%	0.0%	13.6%	100.0%
	Total	60.7%***	8.0%	0.0%	18.8%	30.6%
		28	25	3	16	72
		38.9%	34.7%	4.2%	22.2%	100.0%
		100.0%	100.0%	100.0%	100.0%	100.0%

A2 and B1 types were merged into a single category to achieve <20% of the expected count to be <5.0, and in the *post hoc* evaluation  $Z$ -values were transformed in  $\chi^2$ -values and in  $P$ -values (the Bonferroni correction of significance  $\alpha = 0.05/n$ ,  $\alpha = 0.006$ ).

\* $P < 0.05$ ; \*\* $P < 0.01$ ; \*\*\* $P < 0.001$ .

maxillo-maxillary, 2.14 to 3.35 for the naso-nasal, and 1.12 to 1.19 for the parieto-parietal suture of farm pigs (Burn et al., 2010), which were compatible with a  $LII_{PER}$  of 4.95, 3.26, and 1.04 found, respectively, in the present  $\mu$ CT study (Table 1). Only the fronto-frontal suture, with a  $LII_{PER}$  between 2.57 and 2.62, compared to 1.12 of the present report, showed marked differences. Still, we support the adoption of a common definition of sutural interdigitation even when different imaging techniques are applied. More recently, Maloul et al. measured the interdigitation on the external surface of the bone (Maloul et al., 2013, 2014), as also reported by other studies (Jaslow, 1990; Anton et al., 1992). As a consequence, even though referring to the former work of Rafferty and Herring (1999), their  $II$  was calculated in a different plane, which was more similar to the  $LII_{PAR}$  of the present study. The amount of interdigitation was categorized into three levels by Jasinowski et al. (2010), that is, straight butt-ended ( $II = 1.0$ ), moderate interdigitated ( $II = 2.4$ ), and more complex interdigitated ( $II = 4.1$ ). However, in a following study, those categories were reformulated as low ( $II = 2.3$ ), moderate ( $II = 3.4$ ), and complex ( $II = 4.3$ ) (Maloul et al., 2014). These facts highlight the importance of having a common definition of the  $II$ , and a rational categorization of its amount as well. For these reasons, the present study illustrated a calculation in multiple planes, and also proposed four reference categories, that is, I (from 1.0 to <2.0), II (from 2.0 to <3.0), III (from 3.0 to <4.0), and IV ( $\geq 4.0$ ), based on the average  $LII$  of the entire sutural system; thus, to a certain extent, representative of the variation of the interdigitation of most of the sutures.

In the published literature, sutures have been divided into “facial” and “cranial” (Maloul et al., 2013). Although this categorization is well established for skull bones (Moss and Salentijn, 1969), its applicability to sutures may be questionable. In fact, despite sutures connecting pairs of cranial and facial bones can be identified as “cranial” and “facial,” respectively, sutures connecting facial with cranial bones could not be discriminated. Thus, the present study suggested the additional category of “craniofacial” to identify the latest group. Interestingly, differences were found

among  $LII_{PER}$  for each skull region ( $P = 0.001$ ) (Fig. 3), showing values increasing from cranial (1.74, IQR = 1.88), to craniofacial (3.48, IQR = 2.22), to facial (4.35, IQR = 2.55) ( $P = 0.001$ ), as previously noticed by Maloul et al. (2013).

As the 2D interdigitation can be measured using the  $LII$ , the 2D ossification can be identified by the  $LOI$ . Accordingly, obliteration was described by Persson and Thilander (1977) as the relationship between the obliterated suture length and the total suture length, measured on the histological cross-section, that is, similarly to the  $LOI_{PER}$ . The same definition was adopted by other authors as well (Wehrbein and Yildizhan, 2001; Knaup et al., 2004). Conversely, Hershkovitz et al. (1997) suggested to measure the ossification on the ectocranial surface, that is, more similar to the  $LOI_{PAR}$ . That said, the present study showed that the obliteration was not significantly different among skull regions ( $LOI_{PAR}$ ,  $P = 0.130$ , and  $LOI_{PER}$ ,  $P = 0.214$ ) (Fig. 3) and previous hypothesis from Maloul et al. (2010) mentioning possible higher obliteration in facial compared to cranial sutures could not be confirmed.

Knaup et al. (2004) analyzed the sutural width ( $S_w$ ) of the human maxillo-maxillary suture. However, the evaluation was limited to the perpendicular plane  $S_{wPER}$ . In addition, in the present study, the parallel plane was analyzed as well, and differences were found relative to the skull region ( $P = 0.004$ ). Values of  $S_{wPAR}$  decreased from facial (388  $\mu$ m, IQR = 224  $\mu$ m) and craniofacial (394  $\mu$ m, IQR = 256  $\mu$ m), to cranial (239  $\mu$ m, IQR = 115  $\mu$ m) (Fig. 3), in agreement with the previously reported decrease of interdigitation.

Significant differences were also present between  $LII_{PAR}$  and  $LII_{PER}$  of the same suture ( $P = 0.015$ ), which support the proposed categorization in four types (A1, A2, B1, and B2) (Fig. 2). Most of the sutures with low  $LII$  on both the parallel and perpendicular plane (A1) were present in the neurocranium (77.3%), whereas sutures with higher  $LII$  on both planes (B2) were prevalent in the splanchnocranium ( $P < 0.001$ ).

In addition, sutural interdigitation and ossification may also differ between the endocranial and the ectocranial surface. However, as suggested by Markey and Marshall (2007), the ectocranial surface may not be an accurate

representation of the complex morphology of the suture. Furthermore, its analysis is usually performed through visual assessment, which has limited accuracy compared to histological and radiological methods.

Further parameters have been proposed to offer a 3D measurement of the obliteration, such as the connectivity reported by Maloul et al. (2010) also describable as surface obliteration index (*SOI*). Respectively, a 3D measurement of the interdigitation could be developed, that is, the surface interdigitation index (*SII*). Although such parameters could be relevant for mechanical calculations involving the loaded area, their application in anatomical evaluations may be limited by the lack of comparability with standard 2D techniques, as stated by Maloul et al. (2010). In fact, previous studies adopted a 2D rather than a 3D obliteration index to allow a better and more realistic comparison with former histological analyses (Korbmayer et al., 2007). Furthermore, although the 3D *SII* would show the average interdigitation, it would not represent its variation on different planes, as noticed by previous authors (Maloul et al., 2013), and its capability to speculate on the stress propagation in the craniofacial skeleton may be limited. Whereas, the suture type classification suggested in the present study that is based on the analysis of a parallel and perpendicular plane may be more effective, being also compatible with 2D methods. Overall, such classification may be particularly relevant to describe dynamic sutural development in relationship to loading and independently from embryological factors. For example, structures such as the sphenothmoidal and the sphenoccipital synchondrosis (Tahiri et al., 2014) were characterized by marked anatomical differences despite their similar embryological origin, and the proposed method can easily identify their peculiar anatomical characteristics.

### Limitations

Swine are commonly used for the biomechanical analysis of the skull (Savoldi et al., 2016) and respective sutures (Baumer et al., 2009). However, some species differences do exist, with pigs having the maxillo-premaxillary sutures patent until the adult period, and humans having it ossified earlier (Behrents and Harris, 1991). Additionally, the presence of the naso-premaxillary and zygomatico-lacrimal suture was observed, which are absent in humans. Furthermore, sphenoparietal, frontozygomatic, and sphenozygomatic sutures were absent in the swine.

With regard to the skeletal development, sexual maturity of swine is reached at about 5–6 months (Reiland, 1978), and the 9–12-month-old animal used in this study can be identified as a young-adult, although only first permanent molars were erupted and skeletal growth may not be completed. The choice of a sample with advanced development was coherent with the aim to assess a more representative morphology of sutures. However, the age was approximate and associating sutural morphology to specific developmental stages was beyond the scope of the present study.

Furthermore, the research interest of the present study was limited to the inter-suture variability, and the analysis was focused on a single animal due to the already non-negligible amount of specimens. Inter-subject sampling and variables such as sexual dimorphism were not

considered, and the representativeness of the data with regard to the population should be considered with caution. Accordingly, the statistical analysis was limited by the use of correlated data from the same individual, and the assumption of independent sampling was not fulfilled. Thus, statistics should be interpreted mainly with descriptive purposes.

### CONCLUSIONS

Interdigitation, obliteration, and width represent the main parameters for the morphological characterization of sutures. Hence, their definition and measurement methods should be clear in order to allow appropriate assessment, and proper comparison among studies.

In the swine, morphological parameters varied within the same suture based on the evaluation plane used, and a multiple plane analysis is advisable. With regard to this, the suture type proposed in the present study could be a useful 3D parameter.

The skull region may affect sutural morphology, and sutures should be divided into facial, craniofacial, and cranial. In fact, in the swine, sutures of the cranial region were less complex and with a thinner width compared to sutures of the face.

### ACKNOWLEDGEMENTS

Authors express their gratitude to Mr. Y. Y. Chui (Hard Tissues Laboratory, Faculty of Dentistry, The University of Hong Kong) for his precious collaboration in the acquisition of the  $\mu$ CT data. This publication is part of the PhD Thesis of Dr. Fabio Savoldi at the Faculty of Dentistry, The University of Hong Kong, which was supported by the Hong Kong PhD Fellowship of the Research Grants Council of Hong Kong.

### LITERATURE CITED

- Anton SC, Jaslow CR, Swartz SM. 1992. Sutural complexity in artificially deformed human (*Homo sapiens*) crania. *J Morphol* 214: 321–332.
- Baumer TG, Powell BJ, Fenton TW, Haut RC. 2009. Age dependent mechanical properties of the infant porcine parietal bone and a correlation to the human. *J Biomech Eng* 131:111006.
- Behrents RG, Harris EF. 1991. The premaxillary-maxillary suture and orthodontic mechanotherapy. *Am J Orthod* 99:1–6.
- Burn AK, Herring SW, Hubbard R, Zink K, Rafferty K, Lieberman DE. 2010. Dietary consistency and the midline sutures in growing pigs. *Orthod Craniofac Res* 13:106–113.
- Cohen MM Jr. 2002. Malformations of the craniofacial region: evolutionary, embryonic, genetic, and clinical perspectives. *Am J Med Genet* 115:245–268.
- Corega C, Vaida L, Baciut M, Serbanescu A, Palaghita-Banias L. 2010. Three-dimensional cranial suture morphology analysis. *Rom J Morphol Embryol* 51:123–127.
- Hassan WA, Lees CC. 2014. Facial cleft detected: is the palate normal? *Best Pract Res Clin Obstet Gynaecol* 28:379–389.
- Herring SW. 2008. Mechanical influences on suture development and patency. *Front Oral Biol* 12:41–56.
- Hershkovitz I, Latimer B, Dutour O, Jellema LM, Wish-Baratz S, Rothschild C, Rothschild BM. 1997. Why do we fail in aging the skull from the sagittal suture? *Am J Phys Anthropol* 103:393–399.
- Hou B, Fukai N, Olsen BR. 2007. Mechanical force-induced midpalatal suture remodeling in mice. *Bone* 40:1483–1493.
- Jasinoski SC, Reddy BD, Louw KK, Chinsamy A. 2010. Mechanics of cranial sutures using the finite element method. *J Biomech* 43: 3104–3111.

- Jaslow CR. 1990. Mechanical properties of cranial sutures. *J Biomech* 23:313–321.
- Jayaprakash PT, Srinivasan GJ. 2013. Skull sutures: changing morphology during preadolescent growth and its implications in forensic identification. *Forensic Sci Int* 229:166.e1–166.e13.
- Knaup B, Yildizhan F, Wehrbein H. 2004. Age-related changes in the midpalatal suture. A histomorphometric study. *J Orofac Orthop* 65:467–474.
- Korbmayer H, Schilling A, Puschel K, Amling M, Kahl-Nieke B. 2007. Age-dependent three-dimensional microcomputed tomography analysis of the human midpalatal suture. *J Orofac Orthop* 68:364–376.
- Maloul A, Fialkov J, Hojjat SP, Whyne CM. 2010. A technique for the quantification of the 3D connectivity of thin articulations in bony sutures. *J Biomech* 43:1227–1230.
- Maloul A, Fialkov J, Whyne CM. 2013. Characterization of the bending strength of craniofacial sutures. *J Biomech* 46:912–917.
- Maloul A, Fialkov J, Wagner D, Whyne CM. 2014. Characterization of craniofacial sutures using the finite element method. *J Biomech* 47:245–252.
- Mann RW, Jantz RL, Bass WM, Willey PS. 1991. Maxillary suture obliteration: a visual method for estimating skeletal age. *J Forensic Sci* 36:781–791.
- Markey MJ, Marshall CR. 2007. Linking form and function of the fibrous joints in the skull: a new quantification scheme for cranial sutures using the extant fish *Polypterus endlicherii*. *J Morphol* 268:89–102.
- Moss ML, Salentijn L. 1969. The primary role of functional matrices in facial growth. *Am J Orthod* 55:566–577.
- Nowaczewska W, Ziolkowski G, Dybala B. 2015. Internal morphology of the nonsyndromic prematurely fused sagittal suture in the human skull - a preliminary micro-CT study. *HOMO* 66:399–413.
- Park DH, Yoon SH. 2011. The trans-sutural distraction osteogenesis for 22 cases of craniosynostosis: a new, easy, safe, and efficient method in craniosynostosis surgery. *Pediatr Neurosurg* 47:167–175.
- Persson M, Thilander B. 1977. Palatal suture closure in man from 15 to 35 years of age. *Am J Orthod* 72:42–52.
- Rafferty KL, Herring SW. 1999. Craniofacial sutures: morphology, growth, and in vivo masticatory strains. *J Morphol* 242:167–179.
- Reiland S. 1978. Growth and skeletal development of the pig. *Acta Radiol Suppl* 358:15–22.
- Savoldi F, Tsoi JK, Paganelli C, Matinlinna JP. 2016. Evaluation of rapid maxillary expansion through acoustic emission technique and relative soft tissue attenuation. *J Mech Behav Biomed Mater* 65:513–521.
- Savoldi F, Tsoi JKH, Paganelli C, Matinlinna JP. 2017. Biomechanical behaviour of craniofacial sutures during distraction: an evaluation all over the entire craniofacial skeleton. *Dent Mater* 33:e290–e300.
- Savoldi F, Tsoi JK, Paganelli C, Matinlinna JP. 2018. The biomechanical properties of human craniofacial sutures and relevant variables in sutural distraction osteogenesis: a critical review. *Tissue Eng Part B Rev* 24:25–36.
- Schneider CA, Rasband WS, Eliceiri KW. 2012. NIH Image to ImageJ: 25 years of image analysis. *Nat Methods* 9:671–675.
- Sherick DG, Buchman SR, Goulet RW, Goldstein SA. 2000. A new technique for the quantitative analysis of cranial suture biology. *Cleft Palate Craniofac J* 37:5–11.
- Tahiri Y, Paliga JT, Vossough A, Bartlett SP, Taylor JA. 2014. The spheno-occipital synchondrosis fuses prematurely in patients with Crouzon syndrome and midface hypoplasia compared with age- and gender-matched controls. *J Oral Maxillofac Surg* 72:1173–1179.
- Tome W, Yashiro K, Kogo M, Yamashiro T. 2016. Cephalometric outcomes of maxillary expansion and protraction in patients with unilateral cleft lip and palate after two types of palatoplasty. *Cleft Palate Craniofac J* 53:690–694.
- Trindade-Suedam IK, Castilho RL, Sampaio-Teixeira AC, Araujo BM, Fukushima AP, Campos LD, Trindade IE. 2016. Rapid maxillary expansion increases internal nasal dimensions of children with bilateral cleft lip and palate. *Cleft Palate Craniofac J* 53:272–277.
- Wehrbein H, Yildizhan F. 2001. The mid-palatal suture in young adults. A radiological-histological investigation. *Eur J Orthod* 23:105–114.